

DELPHI Collaboration



DELPHI 99-67 CONF 254

15 June, 1999

Measurement of the single- W production cross-section at LEP2

A. Tonazzo

CERN, CH-1211 Geneva 23, Switzerland

M. Bonesini

INFN, Sezione di Milano, via Celoria 16, IT-20133 Milan, Italy

H.M. Blom, J. Timmermans

NIKHEF, Postbus 41882, NL-1009 DB Amsterdam, The Netherlands

H.T. Phillips

Rutherford Appleton Laboratory, Chilton, Didcot OX11 0QX, UK

PRELIMINARY

Abstract

Preliminary measurements of the cross-sections for single- W production ($e^+e^- \rightarrow e\nu_e W$) have been performed with the data collected by the DELPHI experiment at centre-of-mass energies of 183 and 189 GeV. Both hadronic and leptonic decays of the W boson have been considered: their experimental signature consists of a pair of acoplanar jets or of a single lepton with large transverse momentum. The obtained values are

$$\sigma(e^+e^- \rightarrow e\nu_e W) = .65_{-0.18}^{+0.20} \text{ (stat.)} \pm .05 \text{ (syst.) pb} \quad (\sqrt{s} = 189 \text{ GeV})$$

$$\sigma(e^+e^- \rightarrow e\nu_e W) = .79_{-0.27}^{+0.31} \text{ (stat.)} \pm .05 \text{ (syst.) pb} \quad (\sqrt{s} = 183 \text{ GeV})$$

in agreement with the predictions of the Standard Model.

OPEN-99-419
15/06/1999

1 Introduction

Single W production ($e^+e^- \rightarrow e\nu_e W$, $W \rightarrow f\bar{f}'$) is a good test of the Standard Model, both for the study of the trilinear couplings at the $WW\gamma$ vertex and for the measurement of its cross section. Measurement of the trilinear gauge couplings, both with WW and $W\nu$, are presented by the DELPHI Collaboration in a separate paper [1]. This paper presents preliminary measurements of single- W production cross-sections using the data collected by DELPHI at centre-of-mass energies of 183 and 189 GeV.

The tree-level Feynman diagrams contributing to single- W production at LEP2 are shown in figure 1. Other diagrams lead to the same four-fermion final states $e\nu_e f\bar{f}'$, for example W -pair production. A distinctive feature of the $e^+e^- \rightarrow e\nu_e W$ process is the fact that the distribution of the electron direction is strongly peaked at small angles with respect to the incoming beam direction. We have restricted the definition of our signal to the region of phase space where the contribution of the single- W process is dominant by requiring the outgoing electron to fall below the lower edge of the DELPHI detector acceptance

$$|\cos\theta_{e-}| > .9993$$

(charge conjugation is implied throughout the text). For the $e\nu_e e\nu_e$ final state, a large contribution interfering with the signal is due to the process $e^+e^- \rightarrow Ze^+e^-$ (Zee) with $Z \rightarrow \nu_e\bar{\nu}_e$. In order to reduce it, the signal phase space was further restricted to

$$|\cos\theta_{e+}| < .72$$

$$E_{e+} > 30 \text{ GeV} ;$$

this was taken into account in the definition of the experimental efficiency.

Both hadronic and leptonic decays of the W boson were considered in the analysis. $e\nu_e W \rightarrow e\nu_e q\bar{q}$ events are characterised by the presence of two acoplanar hadronic jets, with a large amount of missing energy due to the undetected neutrino and to the electron escaping along the beam pipe. For the $e\nu_e W \rightarrow e\nu_e l\nu_l$ channel, the experimental signature is a single lepton with large transverse momentum and no other significant energy deposition in the detector.

The analysis was performed on the data samples collected by the DELPHI experiment at centre-of-mass energies of 183 and 189 GeV. The corresponding integrated luminosities are 52 and 154 pb^{-1} respectively.

Signal events were simulated both with the GRC4F [2] and with the PYTHIA [3] Monte Carlo programs. For background processes, different generators were used: EXCALIBUR [4] for the WW and other four-fermion reactions, PYTHIA for $e^+e^- \rightarrow f\bar{f}$, TWOGAM [5] and BDK [6] for two-photon collisions, TEEGG [7] for $e^+e^- \rightarrow e^+e^-\gamma$, KORALZ [8] for $e^+e^- \rightarrow \mu^+\mu^-(\gamma), \tau^+\tau^-(\gamma)$. All the events were processed through the full DELPHI detector simulation and analysis chain [9].

2 Data analysis

2.1 Selection of hadronic events

The experimental signature of $e\nu_e W \rightarrow e\nu_e q\bar{q}$ events consists of a pair of acoplanar jets originating from the hadronic decay of the W . The undetected neutrino results in large

amount of missing energy pointing away from the beam direction.

Other physics processes which can give rise to a similar topology are $e^+e^- \rightarrow Z\gamma$ with $Z \rightarrow q\bar{q}$, WW events with at least one W decaying into hadrons, other four fermion final states ($l^+l^-q\bar{q}$, $\nu\bar{\nu}q\bar{q}$) and two-photon collisions. Some of these processes have cross-sections larger than that of the signal by several orders of magnitude. Sequential cuts on the event variables have been applied to reject them. Table 1 shows the number of selected events in the data at 189 GeV in comparison to the expectation from Monte Carlo at successive stages of the analysis, described in the following.

A sample of hadronic events was preselected by requiring at least 7 charged tracks to be measured in the detector. The contribution from two-photon collisions was reduced by requiring the opening angle of the cone around the beam axis which contains 15% of the visible energy to be larger than 18° : $\gamma\gamma$ events are concentrated in the forward regions and have low values of this variable. Furthermore, the total transverse energy was required to be larger than 16% of \sqrt{s} . This stage of the selection is indicated as “Step 1” in table 1.

	$e\nu_e W$	WW	$Z\gamma$	$\nu\bar{\nu}q\bar{q}$	Others	Data
Step 1	36.3	1392.7	9484.2	29.5	263.8	11550
Step 2	22.6	565.1	503.5	17.3	18.7	1130
Step 3	21.6	146.8	139.0	16.3	15.5	405
Step 4	$14.06 \pm .69$	$21.71 \pm .92$	$5.08 \pm .31$	$8.93 \pm .15$	$.47 \pm .47$	52

Table 1: Number of events expected from the contribution of different channels and observed in the data at different stages of the $e\nu_e W$, $W \rightarrow q\bar{q}$ selection at $\sqrt{s} = 189$ GeV. The column labelled “Others” includes $llq\bar{q}$ final states and two-photon collisions. The steps of the selection are described in the text.

The background from $e^+e^- \rightarrow Z(\gamma)$, $Z \rightarrow q\bar{q}$ was rejected by requiring the effective collision energy $\sqrt{s'}$ [10] to be smaller than $0.85 \cdot \sqrt{s}$ and the polar angle of the missing momentum, θ_{miss} , to be larger than 25° . In addition, since the background is concentrated simultaneously at large $|\cos\theta_{miss}|$ and at values of $\sqrt{s'}$ close to the Z mass, a cut on the correlation of the two variables was applied: $\sqrt{s'} > 160 \cdot |\cos\theta_{miss}| - 30$. $Z(\gamma)$ events in which the ISR photon escaped undetected in the dead region between the barrel and end-cap electromagnetic calorimeters ($\theta \sim 40^\circ$) were suppressed by looking for signals in the hermeticity counters in a cone of 30° around the direction of the missing momentum. Cuts on the visible energy and on the transverse missing momentum were applied as shown in figure 2. (“Step 2” in table 1). Finally, the planarity of the three-body reaction $q\bar{q}\gamma$ was exploited. Two jets were reconstructed with all the detected particles, and their acollinearity was required to exceed 15° . In addition, the stereo angle formed by the two jet axes and the direction of the beam was required to be smaller than 352° . (“Step 3” in table 1).

The most important remaining contribution to the background is due to $e^+e^- \rightarrow W^+W^-$. Events in which both W bosons decay into a $q\bar{q}$ pair tend to have a four-jet topology, and were rejected by requiring the distance parameter for the transition from

3 to 4 jets in the Durham algorithm [11], $D_{3 \rightarrow 4}^{join}$ to be larger than 0.005. When one W decays into $q\bar{q}$ and the other one into $l\nu$, an isolated lepton with high energy is visible: events were rejected if an identified electron or muon was found with an energy larger than 15 GeV and forming an angle of more than 10° from the nearest track. If the lepton is a τ , the direct recognition of its decay products in the hadronic environment is more difficult, thus the 3-jet-like topology of the events was exploited: the $D_{2 \rightarrow 3}^{join}$ for the transition from 2 to 3 jets was required to exceed 0.05. The residual contamination from $q\bar{q}\tau\nu_\tau$ events in which the τ decay products have very low energy or are very close to one of the hadronic jets was reduced by a cut on the maximum transverse momentum of any track with respect to the closest jet, $P_{tr}^{max} < 3.5$ GeV, as shown in figure 3. (“Step 4” in table 1).

As can be seen from the final line of table 1, the main contamination to the final selected sample is due to WW production, with one W decaying into hadrons and the other one into $\tau\nu_\tau$.

The efficiency of the selection on the signal, the expected background and the number of selected events in the data at the two centre-of-mass energies are reported in table 2, together with the evaluated cross section for the hadronic channel alone, $\sigma_{e\nu_e q\bar{q}} = \sigma_{e\nu_e W} \cdot BR(W \rightarrow q\bar{q})$.

\sqrt{s} (GeV)	Efficiency (%)	σ_{backgr} (pb)	\mathcal{L}_{int}	N_{data}	$\sigma_{e\nu_e q\bar{q}}$ (pb)
189	26.2 ± 1.3	$.235 \pm .007$	154.00	52	$.39^{+.19}_{-.17}$
183	31.5 ± 1.5	$.214 \pm .009$	51.85	15	$.24^{+.26}_{-.21}$

Table 2: Performance of the $e\nu_e W$, $W \rightarrow q\bar{q}$ event selection at the two centre-of-mass energies considered in the analysis.

A candidate event for $e^+e^- \rightarrow e\nu_e W$, $W \rightarrow q\bar{q}$ is shown in figure 4.

2.2 Selection of leptonic events

The experimental signature of the leptonic channel $e^+e^- \rightarrow e\nu_e W$, $W \rightarrow l^-\bar{l}$ is the presence of a high energy lepton from the W decay accompanied by a large missing momentum and no other significant energy deposition in the detector. The analysis was optimised for final state leptons that are electrons or muons, and its sensitivity to $W \rightarrow \tau\nu_\tau$ is only marginal.

The main backgrounds for the leptonic channel are radiative production of two leptons $e^+e^- \rightarrow l^+l^-(\gamma)$, $e^+e^- \rightarrow W^+W^-$ events and two-photon collisions.

Events were selected if exactly one well measured charged track was reconstructed. The quality of the track measurement was assessed as follows:

- relative error on the momentum $\Delta P/P < 100\%$;
- track length greater than 20 cm;
- polar angle $\theta > 10^\circ$;

- impact parameter with respect to the primary vertex determined in hadronic events smaller than 4 cm in the transverse plane ($IP_{R\phi}$) and smaller than 3 cm/ $\sin\theta$ along the beam direction (IP_z).

Loose lepton identification criteria were applied, requiring associated hits in the muon chambers or a significant energy deposition in the electromagnetic calorimeter. For electrons, the acceptance was restricted to the barrel region $|\cos\theta| < .72$, and the best determination of the track energy was estimated by combining the momentum measurement from the tracking devices and the calorimetric energy.

Any other energy deposit in the detector not related to the track should not exceed 2 GeV. In addition, the presence of tracks not fulfilling the quality criteria listed above was used to veto the event.

The acceptance was restricted to the kinematic region of W decays by requiring the track momentum to lie between 10% and 45% of \sqrt{s} and its transverse momentum to exceed $12\% \cdot \sqrt{s}$.

A large residual contamination was still present, due to cosmic events in the muon channel and to Compton scattering in the electron channel. The former were suppressed by tightening the cuts on the track impact parameters to $IP_{R\phi} < 0.2$ cm and $IP_z < 2$ cm for the muons. Compton events can mimic the $W \rightarrow e\nu_e$ signal when the photon balancing the electron in the transverse plane is lost in the dead region between the barrel and forward electromagnetic calorimeters, therefore events were rejected if a signal was found in the hermeticity counters in the hemisphere opposite to the track.

Lepton	Eff.(%) on e/μ	Eff.(%) on τ	σ_{bkg} (pb)	\mathcal{L}_{int} (pb $^{-1}$)	N_{data}	$\sigma_{e\nu_e l\nu_l}$ (pb)
$\sqrt{s} = 189$ GeV						
μ	58.8 ± 1.6	2.3 ± 0.5	$.011 \pm .002$	153.45	8	$.24^{+.10}_{-.08}$
e	43.5 ± 1.5	2.3 ± 0.6	$.043 \pm .008$		12	
$\sqrt{s} = 183$ GeV						
μ	58.3 ± 1.4	2.8 ± 0.5	$.012 \pm .002$	51.85	6	$.45^{+.21}_{-.17}$
e	43.2 ± 1.7	2.9 ± 0.8	$.038 \pm .008$		3	

Table 3: Performance of the $e\nu_e W$, $W \rightarrow l\nu$ event selection at the two centre-of-mass energies considered in the analysis.

Figure 5 shows the momentum distribution of single leptons in data and simulation, before applying the cut on this variable.

The performance of the analysis at the two centre-of-mass energy values and the results obtained are reported in table 3. The quoted cross-section refers to the leptonic channel alone: $\sigma_{e\nu_e l\nu} = \sigma_{e\nu_e W} \cdot BR(W \rightarrow l\nu)$. The main contribution to the residual background is due to WW events (10 fb) in the muon channel and to Zee with $Z \rightarrow \nu\nu$ (28 fb) in the electron channel.

As was mentioned above, interference of the signal with the Zee process is relevant in the $e\nu_e e\nu_e$ channel. Its treatment in the computation of the $e\nu_e W$ cross-section is

described in the next section. If the interference is not considered, an effective cross-section for the $e^+e^- \rightarrow e\nu_e e\nu_e$ process within the acceptance cuts defined in section 1 can be computed. At $\sqrt{s} = 189$ GeV, for example, it is found to be $55.{}^{+31}_{-25}$ (stat.) fb, consistent with the expectation of the GRC4F program (25.7 fb).

A candidate event for single W decaying into a muon is shown in figure 6.

3 Extraction of the single-W cross-section

To derive single W production cross sections in the collinear region ($\cos\theta_e > .9993$) the Standard Model branching ratios for W decays were assumed [14]. The effects of interference with other processes leading to the same four-fermion final states were evaluated by comparing the prediction of the GRC4F program, which handles the interference of all diagrams leading to the same final state, with those of PYTHIA, which treats $e\nu_e W$ and Zee separately. A correction factor was included in the definition of the relative contribution of different channels, in analogy to the DELPHI measurement of the $e^+e^- \rightarrow W^+W^-$ cross-section [12].

The following results were obtained

$$\begin{aligned}\sigma(e^+e^- \rightarrow e\nu_e W) &= .65 {}^{+.20}_{-.18} \text{ (stat.) pb} && (\sqrt{s} = 189 \text{ GeV}) \\ \sigma(e^+e^- \rightarrow e\nu_e W) &= .79 {}^{+.31}_{-.27} \text{ (stat.) pb} && (\sqrt{s} = 183 \text{ GeV})\end{aligned}$$

4 Study of systematic uncertainties

The main source of systematic error is due to the limited simulation statistics, both for the signal and for the background.

Possible inaccuracies in the modelling of background processes were evaluated by comparing different Monte Carlo generators. The only significant effect was found in the $q\bar{q}\gamma$ channel, where the background estimate to the hadronic selection using a sample generated with the ARIADNE [13] parton shower treatment was found to be $(6.01 \pm .62)$ events at 189 GeV. The difference from the value obtained from the PYTHIA/JETSET samples quoted above was considered as uncertainty.

The value of the $e^+e^- \rightarrow W^+W^-$ cross-section measured by the LEP experiments on the 189 GeV data [14] was lower than the Standard Model expectation. This discrepancy was taken into account as a systematic uncertainty on the contamination due to WW events.

The total systematic error on the background cross-section due to the effects listed above amounts to 5% in the $q\bar{q}$ channel and 20% in each of the leptonic channels.

From a comparison of dimuon events in data and Monte Carlo, the tracking efficiency ϵ_{track} of DELPHI was found to be overestimated by 0.5% in the simulation [15]. This has a negligible effect on the background, while it affects the selection efficiency on the signal for leptonic decays of the W.

For the $e\nu_e e\nu_e$ channel, an uncertainty of 10% on the evaluation of interference effects between $e\nu_e W$ and Zee was taken into account.

The luminosity is known with a total error of 1%, which leads to the same relative uncertainty on the measured cross-section.

The effect of the uncertainties listed above on the measurement of the total $e^+e^- \rightarrow e\nu_e W$ cross-section at $\sqrt{s}=189$ GeV are reported in table 4. The total systematic error, obtained from the sum in quadrature of the individual contributions, is at the level of 10%. For the measurement at 183 GeV, the same relative error was assumed.

Systematic effect	Error on $\sigma_{e\nu_e W}$ (pb)
$\Delta\sigma_{bkg} (q\bar{q}) \pm 5\%$.031
$\Delta\sigma_{bkg} (e\nu_e) \pm 20\%$.006
$\Delta\sigma_{bkg} (\mu\nu_\mu) \pm 20\%$.012
$\Delta\varepsilon (q\bar{q})$ due to simul. stat.	.015
$\Delta\varepsilon (l\nu)$ due to simul. stat	.017
$\Delta\varepsilon (l\nu)$ due to ε_{track}	.016
Interference effects in $e\nu_e e\nu_e$.004
Luminosity $\pm 1\%$.007
Total	.045

Table 4: Contribution of the uncertainties described in the text to the systematic error on the total $e\nu_e W$ cross-section at $\sqrt{s} = 189$ GeV.

5 Conclusions

The cross-section for single W production has been measured in e^+e^- collisions at 183 and 189 GeV in the centre of mass by the DELPHI Collaboration, obtaining :

$$\sigma(e^+e^- \rightarrow e\nu_e W) = .65^{+.20}_{-.18} \text{ (stat.)} \pm .05 \text{ (syst.) pb} \quad (\sqrt{s} = 189 \text{ GeV})$$

$$\sigma(e^+e^- \rightarrow e\nu_e W) = .79^{+.31}_{-.27} \text{ (stat.)} \pm .05 \text{ (syst.) pb} \quad (\sqrt{s} = 183 \text{ GeV})$$

in agreement with Standard Model expectations.

The results of the analysis are compatible with the ones obtained from a parallel study optimized to the measurement of anomalous gauge boson couplings, presented by DELPHI in a separate paper [1].

The measured cross sections are shown in figure 7, together with the predictions of the GRC4F Monte Carlo.

6 Acknowledgements

We are grateful to O. Ioutschenko, R.Keranen, C.Mariotti and E.Piotto for useful suggestions in the analysis.

References

- [1] DELPHI Collaboration, *Study of Trilinear Gauge Couplings $WWV(V = \gamma, Z)$ at 189 GeV*, paper number 6-360 submitted to this conference
- [2] J.Fujimoto et al., *Comp. Phys. Comm.* 100 (1997) 128
- [3] T.Sjöstrand, *Comp. Phys. Comm.* 39(1986) 347; T.Sjöstrand, *PYTHIA 5.7 and JET-SET 7.4 Physics and Manual*, CERN-TH/7112/93, revised August 1995
- [4] F.A.Berends, R.Pittau and R.Kleiss, *Comp. Phys. Comm.* 85 (1995) 437
- [5] S.Nova, A.Olshevski and T.Todorov, *a Monte Carlo event generator for two-photon physics*, DELPHI 90-35 PROG 152 (1990)
- [6] F.A.Berends, P.H.Daverveldt and R.Kleiss, *Comp. Phys. Comm.* 40 (1986) 271, 285, 309
- [7] D.Karlen, *Nucl. Phys. B* 289 (1987) 23
- [8] S.Jadach, J.H.Kühn and Z.Was, *Comp. Phys. Comm.* 79 (1994) 503
- [9] *DELSIM Reference Manual*, DELPHI 87-97 PROG 100 (1987); *DELPHI Data Analysis Program (DELANA) User's Guide*, DELPHI 89-44 PROG 137 (1989)
- [10] P.Abreu et al., *Nucl. Instr. Meth.* A427 (1999) 497
- [11] S.Catani, *The k_T algorithm for jet production and fragmentation*, CERN-TH.6895/93 (1993)
- [12] DELPHI Collaboration, P.Abreu et al., *Phys. Lett. B* 397 (1997) 158
- [13] L.Lönnblad, *Comp. Phys. Comm.* 71 (1992) 15
- [14] ALEPH Collaboration, *WW cross section and W branching ratios at $\sqrt{s} = 189$ GeV*, ALEPH 99-020 CONF 99-015 (1999);
P.Buschmann et al., *Measurement of the W-pair Production Cross-section and W Branching Ratios at $\sqrt{s} = 189$ GeV*, DELPHI 99-39 MORIO CONF 238 (1999);
L3 Collaboration, *Preliminary Results on the Measurement of W-Pair Production in e^+e^- interactions at $\sqrt{s} = 189$ GeV and W-Decay Branching Fractions*, L3 Note 2376 (1999);
OPAL Collaboration, *W^+W^- Production in e^+e^- Collision at 189 GeV*, OPAL-PN378 (1999)
- [15] P.Renton, private communication.

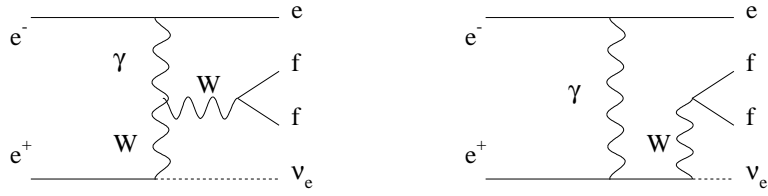


Figure 1: Feynman diagrams contributing to $e^+e^- \rightarrow e\nu_e W$ at lowest order.

DELPHI PRELIMINARY

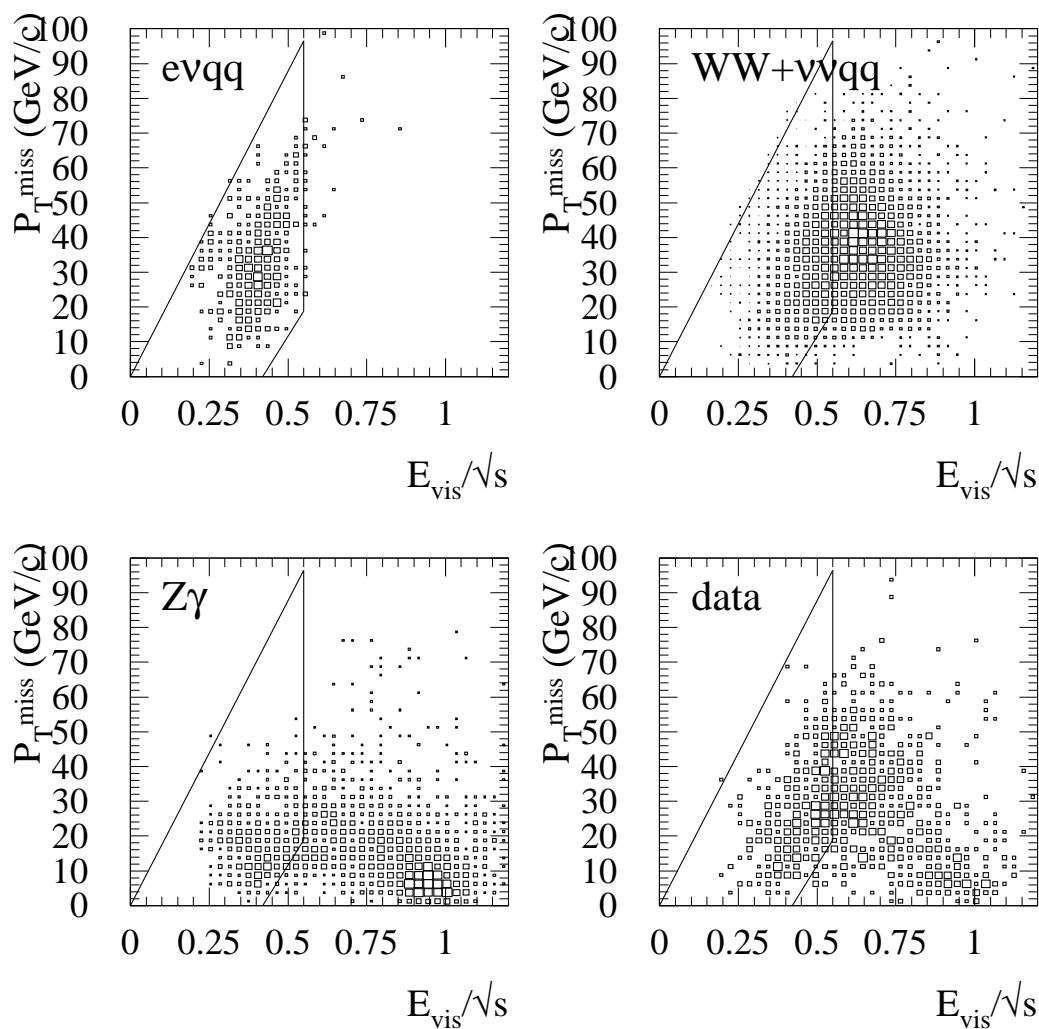


Figure 2: Scatter plot of visible energy and transverse missing momentum for the signal, the main backgrounds and the real data. The region enclosed by the lines is the one accepted in the event selection. The cuts described in the text before the current one have been applied.

DELPHI PRELIMINARY

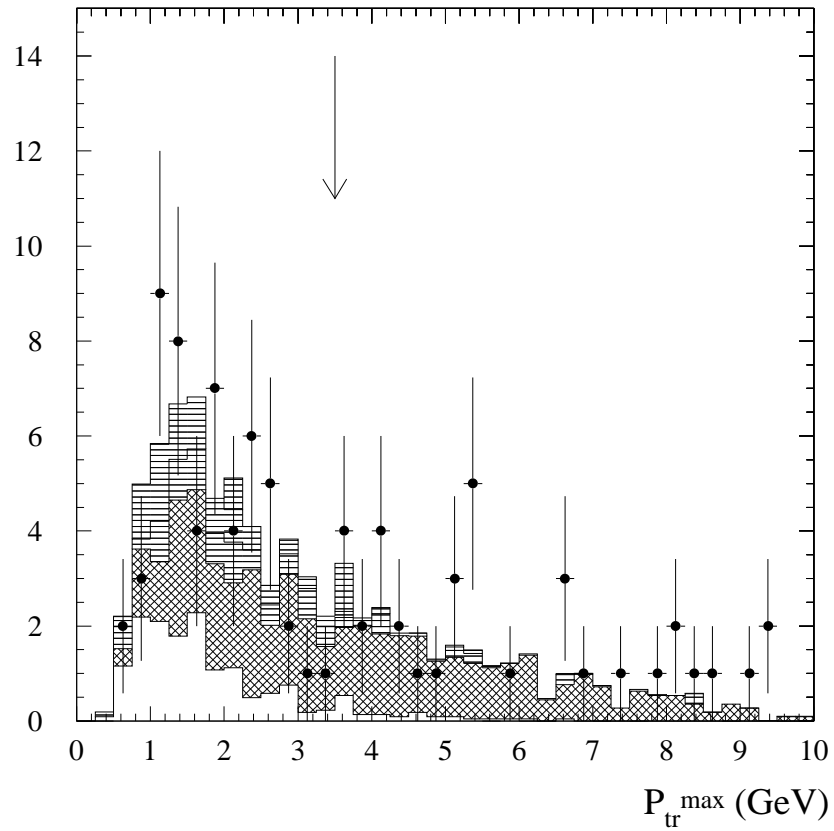



Figure 3: Maximum transverse momentum of any track with respect to the closest jet. The white histogram represents the simulated $e\nu qq$ signal, the cross-hatched area represents the WW background, the other backgrounds are shown with single hatching. Data points at $\sqrt{s} = 189$ GeV are indicated with statistical error bars. All the other selection cuts described in the text have already been applied. The arrow indicates the position of the cut on this variable.

	DELPHI	Run :	87920	Evt :	5327						
		Beam:	94.6 GeV		Proc:	29-Nov-1998	Act				
		DAS:	12-Sep-1998		Scan:	28-Jun-1999					
			21:22:14		Tan+DST						

	TD	TE	TS	TK	TV	ST	PA
Act	0	252	0	42	0	0	0
	(0	X252	X	0	X	42	X
							0
Deact	0	0	0	0	0	0	0
	(0	X	0	X	0	X	5
							0
							X
							0

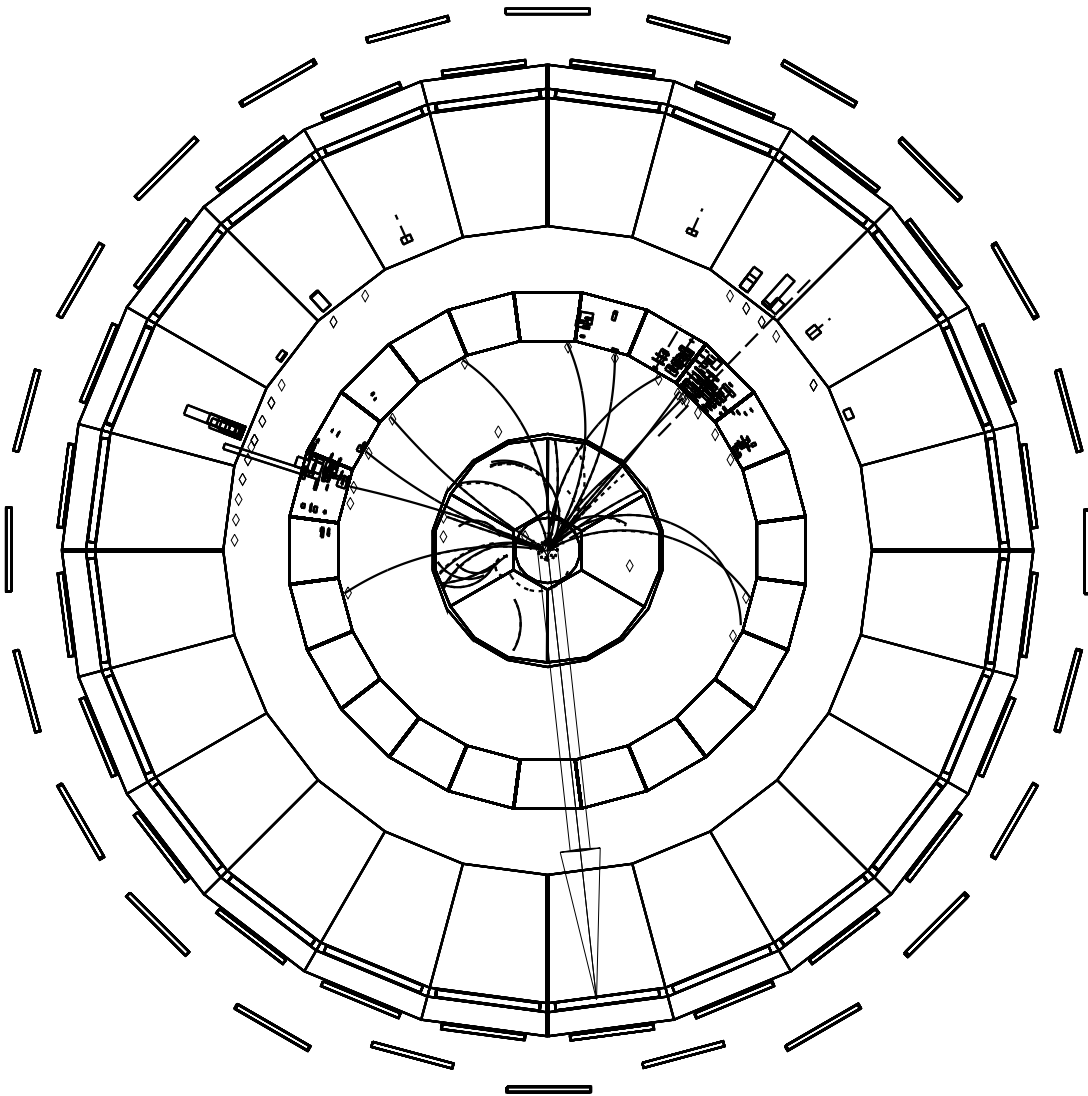


Figure 4: Candidate event for $e^+e^- \rightarrow e\nu_e W$, $W \rightarrow q\bar{q}$. The arrow represents the missing momentum vector.

DELPHI PRELIMINARY

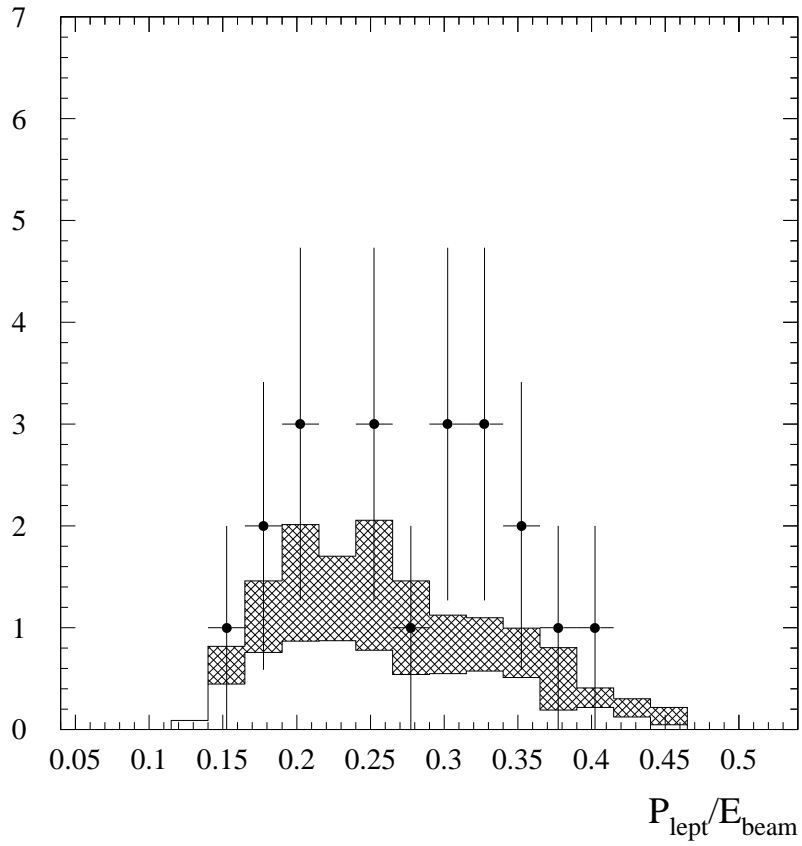



Figure 5: Momentum distributions of selected single lepton events in real data at 189 GeV (points with error bars) and in the simulation (histogram). The open area represents the single-W signal, the cross-hatched histogram is the background expectation.

	DELPHI	Run :	86337	Evt :	22427																		
		Beam:	94.6 GeV	Proc:	23-Nov-1998	Act																	
		DAS:	9-Aug-1998	Scan:	28-Jun-1999		0	115	0	1	0	0	0										
			22:39:44		DST		(0)	(115	X	0)	(1	X	0	X	0	X	0)
						Deact	0	0	0	0	0	0	0	0	0	0	0	0	0	0	0	0	
							(0	X	0	X	0	X	0	X	0	X	0	X	0	X	0)

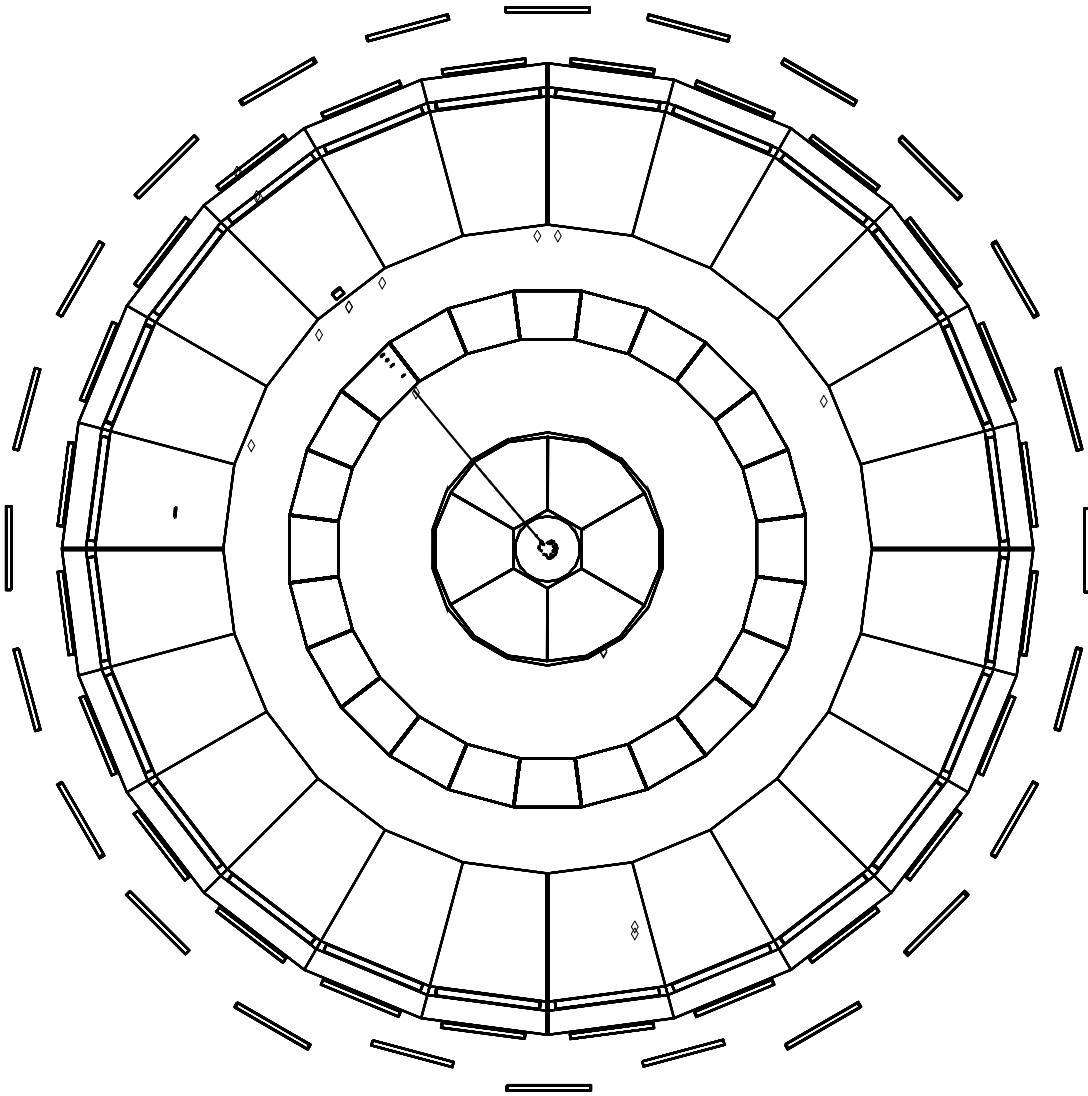


Figure 6: Candidate event for $e^+e^- \rightarrow e\nu_e W, W \rightarrow \mu\nu$.

DELPHI PRELIMINARY

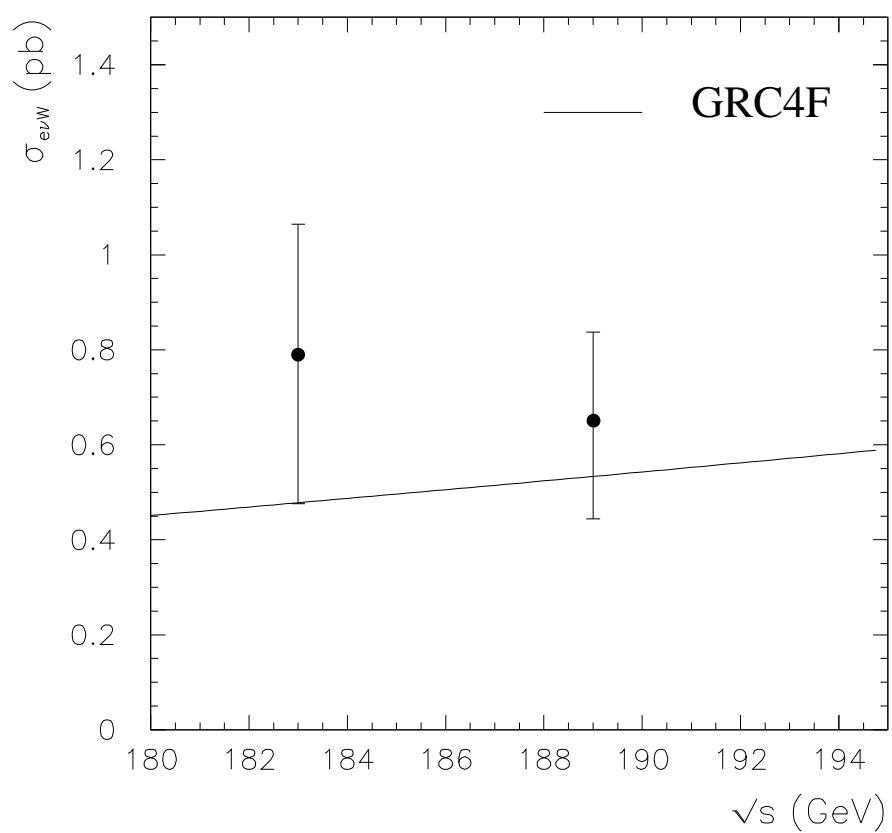


Figure 7: Measured cross-section for single W production, compared with the predictions of the GRC4F Monte Carlo.